

Ammonia adsorption by AI-MIL-53-TDC: performance evaluation and mechanistic study

Xiaona Wang^{a,1}, Hong Wen^{b,1}, Shenghan Wu^a, Guowang Xiao^a, Li Wei^{a,*}, Jingai
Hao^{a,*}

^a Faculty of Light Industry and Chemical Engineering, Dalian Polytechnic
University, Dalian 116034, Liaoning, China

^b Dalian Institute of Chemical Physics, Chinese Academy of Sciences (CAS),
Dalian 116023, Liaoning, China.

¹ These authors contributed equally to this work.

*Corresponding authors:

E-mail address: weili@dlpu.edu.cn (L. Wei), haoja@dlpu.edu.cn (J. Hao)

Experimental section

Materials

2,5-thiophene-dicarboxylic acid (H_2TDC , 98%), aluminum chloride hexahydrate ($\text{AlCl}_3 \cdot 6\text{H}_2\text{O}$, 98%), and N,N-dimethylformamide ($\text{C}_3\text{H}_7\text{NO}$, 99.7%, DMF) were purchased from Shanghai Aladdin Biochem Technology Ltd. The ammonia gas used in this work was obtained from Dalian Junfeng Gas Chemical Co, Ltd.

Synthesis of Al-MIL-53-TDC

The synthesis of Al-MIL-53-TDC is based on literature report.¹ A mixture of $\text{AlCl}_3 \cdot 6\text{H}_2\text{O}$ (64 mg, 0.48 mmol) and H_2TDC (62 mg, 0.36 mmol) was dissolved in 1.8 ml of DMF and 2.5 ml of H_2O . The resultant mixture was then loaded into a polytetrafluoroethylene (PTFE) liner, sealed in a stainless steel reactor, and heated at 100°C for 5 hours. The synthetic product was mixed with DMF and heated to 150°C for 1 hour, followed by the removal of DMF molecules through acetone exchange and drying at 80°C for 24 hours to yield Al-MIL-53-TDC powder.

Gas adsorption and desorption

The adsorption of ammonia was measured using a gravimetric method. The flow of ammonia gas was controlled and introduced into a small vial containing the material. As the gas passed through, the mass of the sample continuously increased until it reached a constant weight, indicating that adsorption had saturated. The residual gas was absorbed by subsequent

acids and water to prevent air pollution. The desorption of ammonia involved heating the adsorbed sample in a vacuum drying oven at 120°C for 2 hours.

Under room temperature, NH₃ absorption in a humid environment was tested using an NH₃ solution vapor atmosphere, and the corresponding NH₃ adsorption was determined by ion chromatography (ICS-5000).²

Characterizations of the MOFs

XRD measurements were conducted using the Shimadzu XRD-7000S in the range of 5° to 60°. SEM images and EDS images (X-MAX50) were captured using the JSM-7800F. Testing was conducted on a TA thermogravimetric analyzer (DSCQ2000) within a temperature range of 25°C to 650°C, with a heating rate of 10°C/min. Ammonium ion content was determined using the Thermo Fisher Scientific ICS-5000+. X-ray photoelectron spectra were recorded using a Thermo Scientific K-Alpha, with the X-ray excitation source being Al K α (1486.6 eV). The N₂ adsorption isotherms were measured at 77 K using a Micromeritics ASAP 2460 volumetric gas adsorption analyzer, and the samples were degassed at 200°C for 6 hours prior to measurement. The specific surface area of the MOFs was calculated using the Brunauer-Emmett-Teller (BET) method. The pore size distribution data were calculated using the Horváth-Kawazoe (HK) method. NH₃-TPD measurements were conducted using a Chemisorption Analyzing System 5080. FT-IR spectra were recorded using an ANTARISII spectrometer with a wavelength range of 400–4000 cm⁻¹.

DFT calculations

DFT calculations were carried out using the CP2K code. A mixed Gaussian and planewave basis sets were employed to the calculations. Core electrons were represented with norm-conserving Goedecker-Teter-Hutter pseudopotentials, and the valence electron wavefunction was expanded in a double-zeta basis set with polarization functions along with an auxiliary plane wave basis set with an energy cutoff of 400 Ry. The generalized gradient approximation exchange-correlation functional of Perdew, Burke, and Enzerhof (PBE) was used. Each configuration was optimized with the OT algorithm with the Broyden-Fletcher-Goldfarb-Shanno (BGFS) algorithm with SCF convergence criteria of 3×10^{-6} au. To compensate the long-range van der Waals dispersion interaction between the adsorbate and the MOFs, the DFT-D3 scheme with an empirical damped potential term was added into the energies obtained from exchange-correlation functional in all calculations. The supercell of TDC was modeled using $1 \times 2 \times 2$ unit cell.

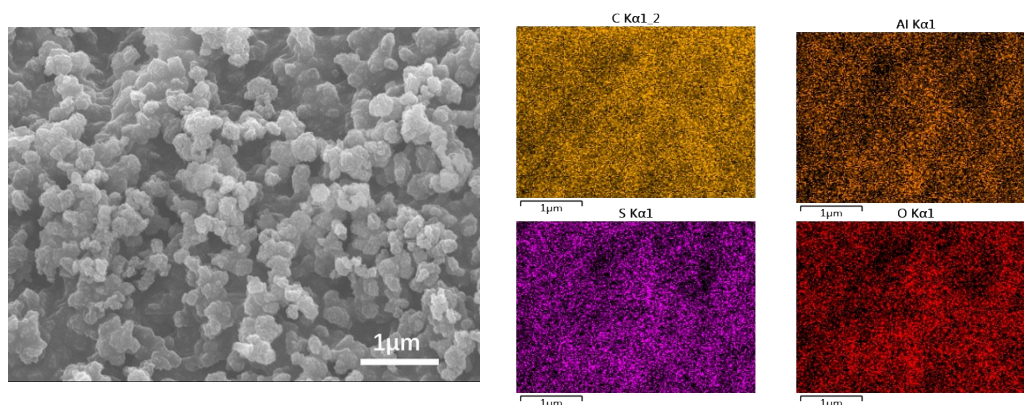


Fig. S1 SEM image and EDS elemental mapping images of Al-MIL-53-TDC.

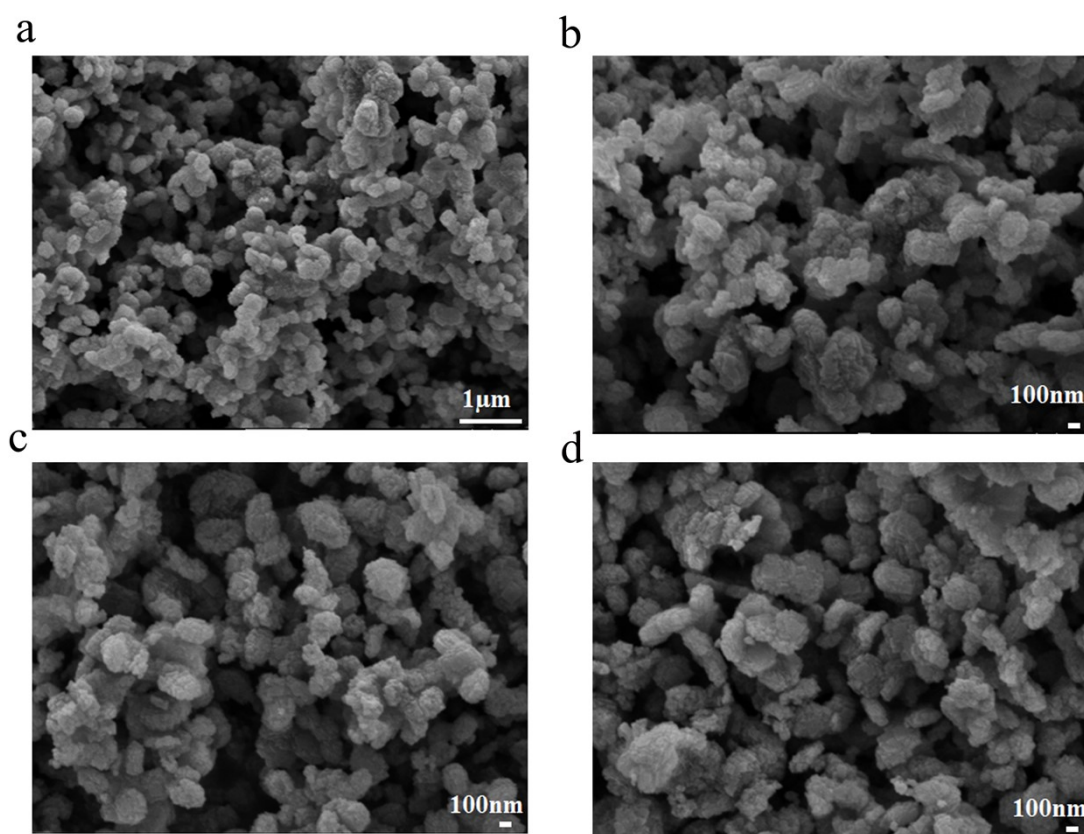


Fig. S2 (a)-(b) SEM images of Al-MIL-53-TDC at different magnifications; (c) SEM image of Al-MIL-53-TDC after ammonia gas adsorption; (d) SEM image of Al-MIL-53-TDC after ammonia desorption.

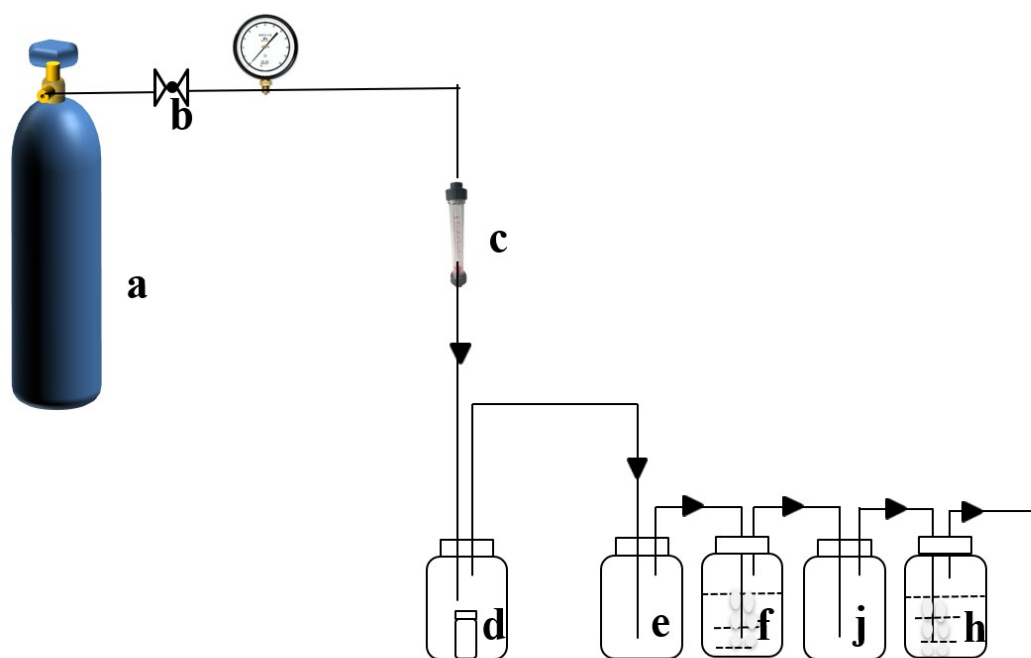


Fig. S3 Schematic diagram of gas absorption apparatus: (a) NH_3 gas cylinder; (b) Pressure reducing valves; (c) Gas rotor flowmeters; (d) Sample bottle; (f) Temperature sensor; (h) Sample bottle; (e and j) Empty bottles; (f) Liquid paraffin; (h) Water.

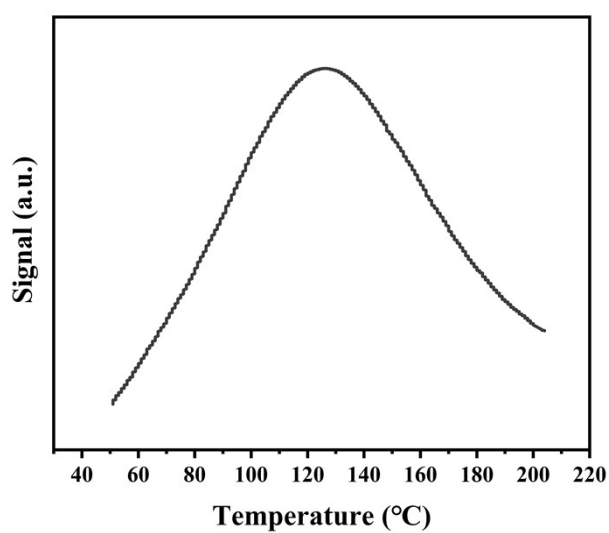


Fig. S4 NH_3 -TPD profile of Al-MIL-53-TDC.

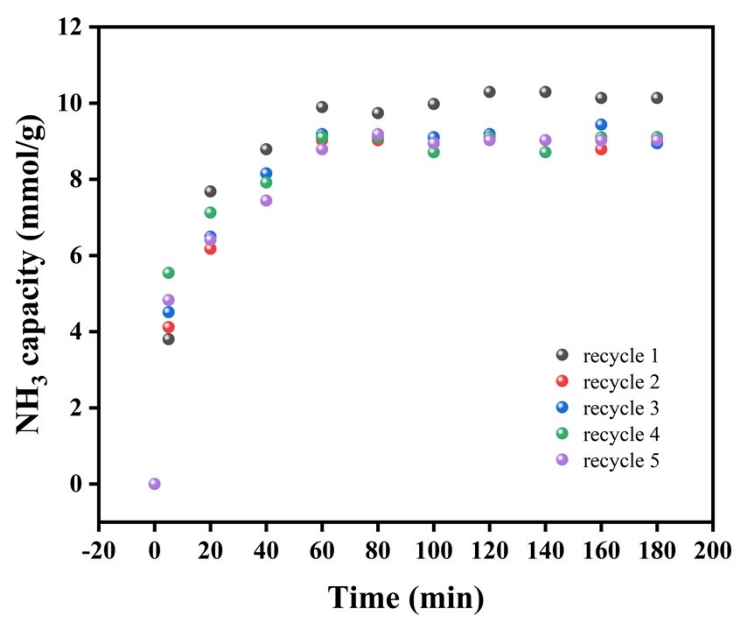


Fig. S5 Kinetics of ammonia adsorption of five recycles.

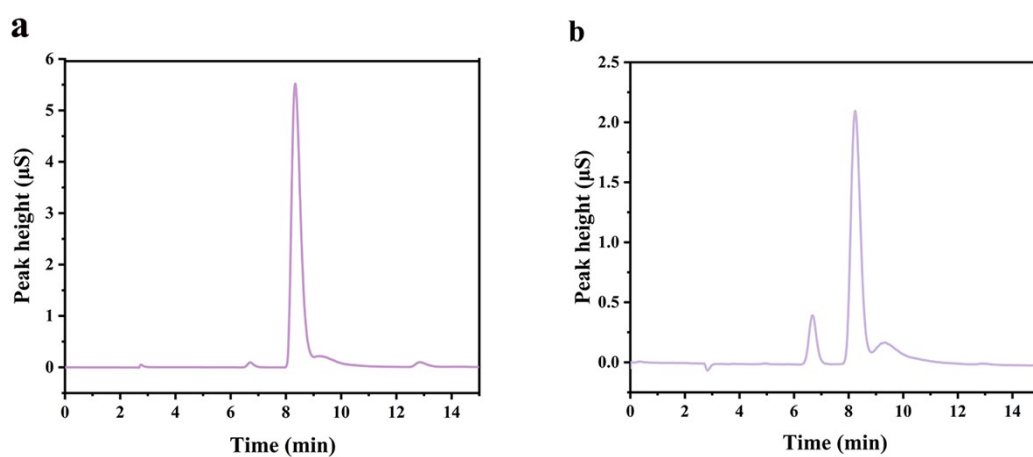


Fig. S6 Ion chromatograms of NH_4^+ under (a) 25% ammonia solution; (b) 10% ammonia solution.

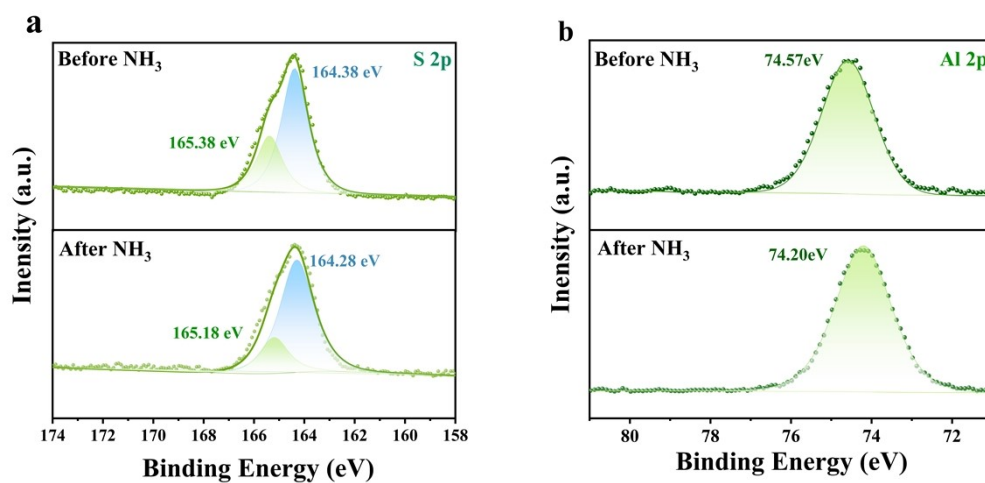


Fig. S7 XPS spectra of S 2p (a) and Al 2p (b) before and after NH_3 adsorption.

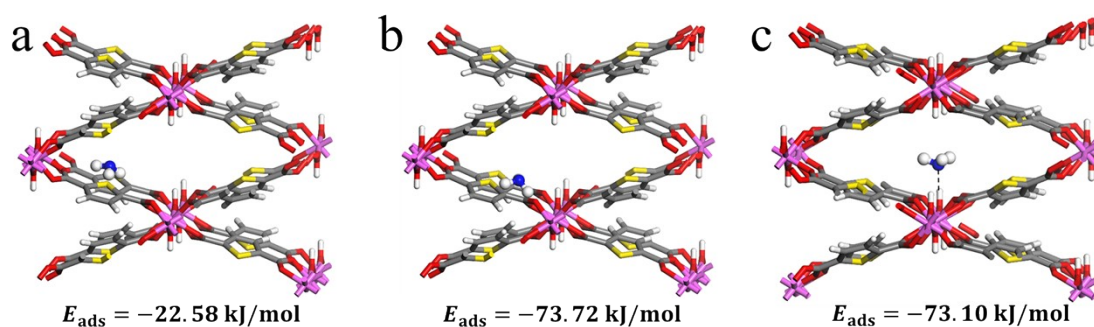


Fig. S8 Optimized structures after NH_3 adsorption: (a) H in NH_3 adsorbed onto S site; (b) one H in NH_3 adsorbed onto S site, another H onto carboxylate O; (c) N in NH_3 adsorbed onto $\mu\text{-OH}$.

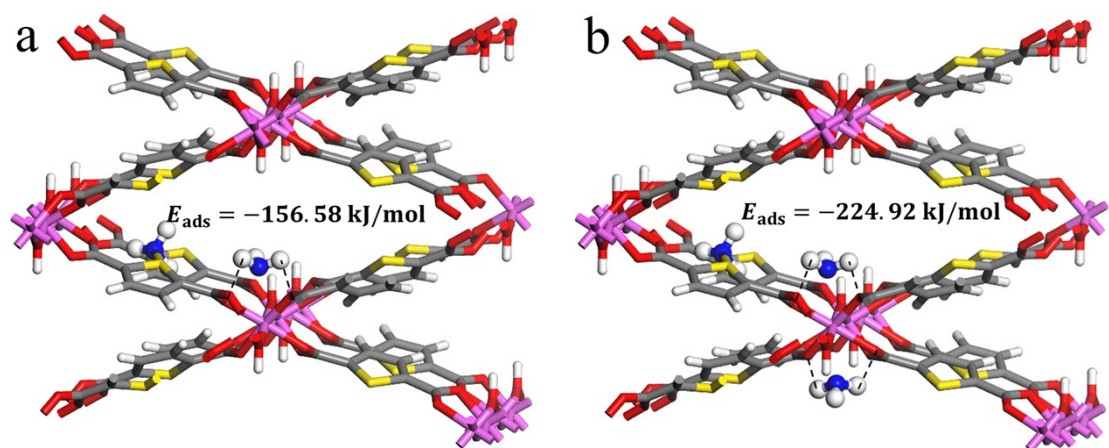


Fig. S9 Optimized structures after NH_3 adsorption: (a) two NH_3 molecules adsorbed;
(b) three NH_3 molecules adsorbed.

Table S1. Comparison of NH₃ adsorption capacities of different MOFs.

| Sample | NH ₃ capacity (mmol/g) | Adsorption Condition | References |
|--------------------------------------|-----------------------------------|----------------------|------------|
| Al-MIL-53-TDC | 12.6 | 25.0 °C, 1.0 bar | This work |
| MOF-5 | 12.2 | 25.0 °C, 1.0 bar | 3 |
| MOF-303(Al) | 19.7 | 25.0 °C, 1.0 bar | 4 |
| Co ₂ Cl ₂ BBTA | 18.0 | 25.0 °C, 1.0 bar | 5 |
| MIL-101-Cr | 10 | 25.0 °C, 1.0 bar | 6 |
| MIL-53 | 4.4 | 25.0 °C, 1.0 bar | 6 |
| NH ₂ -MIL-53-Al | 5.4 | 25.0 °C, 1.0 bar | 6 |
| Mg-MOF-74 | 7.6 | 25.0 °C, 1.0 bar | 7 |
| HKUST-1 | 12.1 | 25.0 °C, 1.0 bar | 8 |
| DUT-6 | 12 | 25.0 °C, 1.0 bar | 9 |
| NU-1401 | 8.41 | 25.0 °C, 1.0 bar | 10 |
| NU-300 | 8.28 | 25.0 °C, 1.0 bar | 11 |
| UiO-66-C | 8.27 | 25.0 °C, 1.0 bar | 12 |
| Ga-PMOF | 10.50 | 25.0 °C, 1.0 bar | 13 |
| Al-PMOF | 7.67 | 25.0 °C, 1.0 bar | 13 |

References

1. C. B. L. Tschense, N. Reimer, C.-W. Hsu, H. Reinsch, R. Siegel, W.-J. Chen, C.-H. Lin, A. Cadiau, C. Serre, J. Senker and N. Stock, *Zeitschrift für anorganische und allgemeine Chemie*, 2017, **643**, 1600-1608.
2. Y. Chen, C. Yang, X. Wang, J. Yang, K. Ouyang and J. Li, *Journal of Materials Chemistry A*, 2016, **4**, 10345-10351.
3. D. Saha and S. Deng, *Journal of Colloid and Interface Science*, 2010, **348**, 615-620.
4. Z. Wang, Z. Li, X.-G. Zhang, Q. Xia, H. Wang, C. Wang, Y. Wang, H. He, Y. Zhao and J. Wang, *ACS Applied Materials & Interfaces*, 2021, **13**, 56025-56034.
5. A. J. Rieth and M. Dincă, *Journal of the American Chemical Society*, 2018, **140**, 3461-3466.
6. Y. Chen, F. Zhang, Y. Wang, C. Yang, J. Yang and J. Li, *Microporous and Mesoporous*

- Materials*, 2018, **258**, 170-177.
7. M. J. Katz, A. J. Howarth, P. Z. Moghadam, J. B. DeCoste, R. Q. Snurr, J. T. Hupp and O. K. Farha, *Dalton Transactions*, 2016, **45**, 4150-4153.
8. C. Petit, L. Huang, J. Jagiello, J. Kenvin, K. E. Gubbins and T. J. Bandosz, *Langmuir*, 2011, **27**, 13043-13051.
9. I. Spanopoulos, P. Xydias, C. D. Malliakas and P. N. Trikalitis, *Inorganic Chemistry*, 2013, **52**, 855-862.
10. Y. Zhang, X. Zhang, Z. Chen, K.-i. Otake, G. W. Peterson, Y. Chen, X. Wang, L. R. Redfern, S. Goswami, P. Li, T. Islamoglu, B. Wang and O. K. Farha, *ChemSusChem*, 2020, **13**, 1710-1714.
11. Y. Chen, X. Zhang, K. Ma, Z. Chen, X. Wang, J. Knapp, S. Alayoglu, F. Wang, Q. Xia, Z. Li, T. Islamoglu and O. K. Farha, *ACS Applied Nano Materials*, 2019, **2**, 6098-6102.
12. W. Morris, C. J. Doonan and O. M. Yaghi, *Inorganic Chemistry*, 2011, **50**, 6853-6855.
13. S. Moribe, Z. Chen, S. Alayoglu, Z. H. Syed, T. Islamoglu and O. K. Farha, *ACS Materials Letters*, 2019, **1**, 476-480.